

*In situ* photoelectron spectroscopy study of water adsorption on model biomaterial surfaces

This article has been downloaded from IOPscience. Please scroll down to see the full text article.

2008 J. Phys.: Condens. Matter 20 184024

(<http://iopscience.iop.org/0953-8984/20/18/184024>)

View [the table of contents for this issue](#), or go to the [journal homepage](#) for more

Download details:

IP Address: 129.252.86.83

The article was downloaded on 29/05/2010 at 11:58

Please note that [terms and conditions apply](#).

# *In situ* photoelectron spectroscopy study of water adsorption on model biomaterial surfaces

G Ketteler<sup>1</sup>, P Ashby<sup>2</sup>, B S Mun<sup>3,4</sup>, I Ratera<sup>5</sup>, H Bluhm<sup>6</sup>, B Kasemo<sup>1</sup>  
and M Salmeron<sup>2,5</sup>

<sup>1</sup> Chalmers University of Technology, Department of Applied Physics, 41296 Gothenburg, Sweden

<sup>2</sup> Molecular Foundry, Lawrence Berkeley National Laboratories, Berkeley, CA 94720, USA

<sup>3</sup> Advanced Light Source, Lawrence Berkeley National Laboratories, Berkeley, CA 94720, USA

<sup>4</sup> Department of Applied Physics, Hanyang University, Ansan, Kyunggi-Do 426-791, Korea

<sup>5</sup> Materials Science Division, Lawrence Berkeley National Laboratories, Berkeley, CA 94720, USA

<sup>6</sup> Chemical Sciences Division, Lawrence Berkeley National Laboratories, Berkeley, CA 94720, USA

Received 10 July 2007, in final form 13 September 2007

Published 17 April 2008

Online at [stacks.iop.org/JPhysCM/20/184024](http://stacks.iop.org/JPhysCM/20/184024)

## Abstract

Using *in situ* photoelectron spectroscopy at near ambient conditions, we compare the interaction of water with four different model biomaterial surfaces: self-assembled thiol monolayers on Au(111) that are functionalized with methyl, hydroxyl, and carboxyl groups, and phosphatidylcholine (POPC) lipid films on silicon. We show that the interaction of water with biomaterial surfaces is mediated by polar functional groups that interact strongly with water molecules through hydrogen bonding, resulting in adsorption of 0.2–0.3 ML water on the polar thiol films in 700 mTorr water pressure and resulting in characteristic N 1s and P 2p shifts for the POPC films. Provided that beam damage is carefully controlled, *in situ* electron spectroscopy can give valuable information about water adsorption which is not accessible under ultrahigh vacuum conditions.

(Some figures in this article are in colour only in the electronic version)

## 1. Introduction

The molecular nature of adsorption at biomaterial surfaces is poorly understood although adsorption of gases, aerosols, and ions and molecules from solution is of fundamental importance at all kind of tissue surfaces. Fundamental questions such as the structure and hydrogen-bonding configuration of water, the chemical binding to the interface, and the extent of water dissociation at a biomaterial surface are largely unknown. Understanding these interactions is a foundation upon which further studies are built in order to understand, e.g. protein folding, conformational changes of proteins by hydrophobic self-assembly, and basic biological and colloidal interactions [1, 2].

Surface sensitive spectroscopy offers the possibility to gain insights into specific adsorption sites, adsorption and

desorption energetics, H-bonding configurations, diffusion and reaction of gases, etc at a submolecular or single-molecule level. High resolution surface sensitive studies are typically performed under ultrahigh vacuum conditions (with the exception of a few techniques such as atomic force microscopy (AFM) or sum frequency generation (SFG)), i.e., at conditions which are not compatible with and relevant in biological environments. Important progress has been made in the field of so called *in situ* techniques that allow atomic scale, surface sensitive investigations during chemical reactions, at the solid–liquid interface, and in equilibrium with vapor close to ambient conditions<sup>7</sup>. New developments and experimental approaches are no longer limited to the solid–gas (or solid–vacuum) interface in UHV conditions

<sup>7</sup> See the other contributions to this issue.

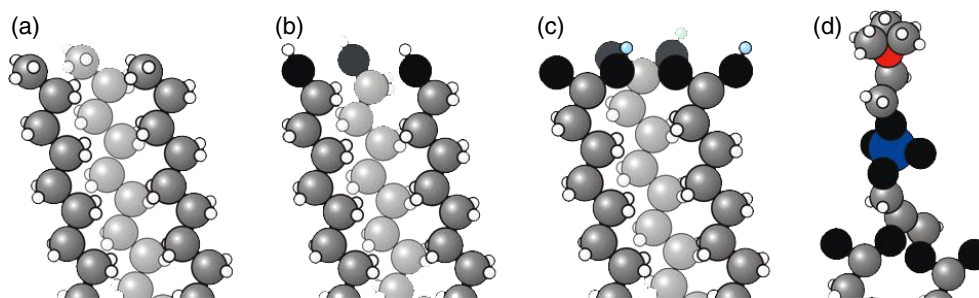


**Figure 1.** Schematic drawings of the different types of biomaterial functional units that were studied by *in situ* photoelectron spectroscopy in the presence of water vapor. (a)–(c) Self-assembled thiol monolayer films on Au(111) with functionalized surfaces (CH<sub>3</sub>-, OH-, and COOH-groups, respectively). (d) The phosphocholine headgroup of a POPC lipid molecule.

(<10<sup>-6</sup> mbar pressure). In combination with the high brilliance of Synchrotron radiation sources, the photon based techniques (XPS, NEXAFS, etc) offer a new way to investigate biological systems.

During the past years, the desire to study biological surfaces with the resolution of typical surface science techniques has triggered the development of model systems that mimic biological surfaces by reducing the complex surface structure to a few functionalities that are immobilized on a suitable substrate. We will present recent results on two different model systems: Functionalized alkanethiol self-assembled monolayers (SAM) on gold as a model system for organic functional groups at the surface of biomolecules [3–8], and supported lipid bilayers (SLB) of phospholipid molecules as a biological model membrane [9, 10] (figure 1). These systems represent very flexible and rich model systems of different biomaterial functionalities and are among the best investigated model systems. While SAMs have been studied in great detail in ultrahigh vacuum (UHV) with surface sensitive techniques, SLBs have been mostly assessed in solution with probes that yield only limited information at the atomic level. We will not discuss the possibility of water interactions at the gold or silicon interface. As we will show below for the hydrophobic film termination no water adsorbs at the interface under the conditions presented in this study.

## 2. Experimental details

### 2.1. Preparation of the films

We used 1-mercaptohexadecane, 11-mercaptoundecanol, and 11-mercaptoundecanoic acid for the preparation of the functionalized self-assembled monolayer films on gold coated glass or mica substrates. The glass substrates were cleaned by ultrasonic immersion in methanol, chloroform, and ethanol, and cleaned in piranha solution. They were rinsed with Millipore water and ethanol. Gold on mica substrates were used directly from the evaporator. Finally, the substrates were annealed with a butane torch to enhance preferential (111) orientation. The substrate flatness and quality was checked with atomic force microscopy (AFM). Then, the substrates were immersed for 24 h in to a 1 mM solution of the substances in ethanol. After this period, they were rinsed with ethanol and dried in a flow of pure nitrogen gas.

Palmitoyl-oleoyl phosphatidylcholine (POPC, Avanti Polar Lipids Inc.) lipid films were deposited on a Si wafer. The wafer was cleaned by immersion into sodium dodecylsulfate, rinsing with Milli-Q water and ethanol, blow dried with N<sub>2</sub>, and oxidized by UV/O<sub>3</sub> for 30 min. The POPC lipids were dissolved in chloroform, deposited onto a Si wafer where the chloroform was evaporated by blowing dry N<sub>2</sub> over the wafer. This procedure results in a disordered multilayer POPC lipid film. The defined deposition and handling of a supported lipid bilayer in ultrahigh vacuum chambers requires strong modifications of the experimental set-up and is not subject of the present study. An ultrahigh vacuum (UHV) chamber dedicated for spectroscopic studies of lipid bilayers is being built in our laboratory at Chalmers University.

### 2.2. Ambient pressure photoemission at the advanced light source (ALS)

Water adsorption studies were performed at beamlines 9.3.2 and 11.0.2 of the advanced light source, Berkeley, USA. Both beamlines are equipped with an ambient pressure photoemission endstation that enables x-ray photoelectron spectroscopy (XPS) measurements in equilibrium with gas pressures up to a few Torr [11, 12]. *In situ* measurements in elevated pressures are enabled by a differential pumping system that separates the elevated pressure chamber from the ultrahigh vacuum (UHV) in the analyzer. The differential pumping section is equipped with an electrostatic lens system for refocusing of the photoelectrons into the object plane of the analyzer.

XPS peaks were deconvoluted by Gauss–Lorentz profiles after subtraction of a linear background and normalized by the incident photon flux and energy-dependent x-ray absorption cross sections [13]. The C 1s and O 1s core levels of the different SAMs used in this study are shown in figure 2. All binding energies were calibrated to the Au 4f core level at 84.0 eV. The determined C 1s and O 1s positions agree well with previously reported binding energy positions for CH<sub>2</sub>, OH, and COOH moieties [14, 15]. Aliphatic CH<sub>2</sub>-groups produce a peak at about 285 eV. The C 1s core level of the carboxyl carbon atom of the COOH-group shows up at 289.2–288.5 eV. The C 1s of the C–OH bond in alcoholic SAMs occurs at 286.4–7 eV. The O 1s core level due to the OH-group in the alcohol-terminated SAM occurs at 532.9 eV.

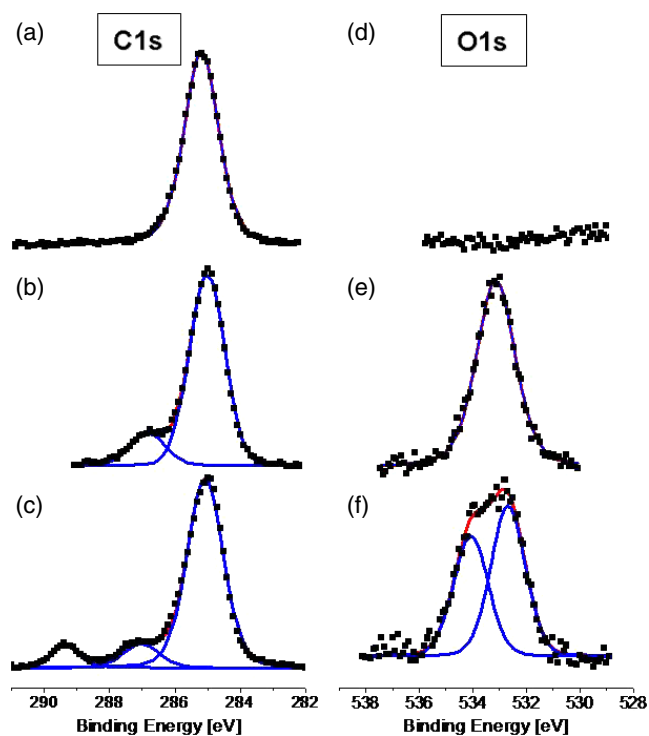


**Figure 2.** C 1s (550 eV) and O 1s (780 eV) core level spectra, respectively, of self-assembled monolayers of (a), (d) mercaptohexadecane, (b), (e) 11-mercaptoundecanol, and (c), (f) 11-mercaptoundecanoic acid.

The O 1s core level of both oxygen atoms in the COOH-group are inequivalent [16, 17]. The double-bonded oxygen has a peak at 532.3 eV, and the OH has a peak at 533.7 eV. From the O 1s core level, we are thus able to calculate the degree of protonation which is about 80% after rinsing with ethanol. Adsorbed water typically shows up as a broad peak at a binding energy of 533–534.5 eV.

Water coverage is given relative to the O 1s intensity of the COOH- or OH-functional group, respectively. One monolayer of thiol molecules in a  $\sqrt{3} \times \sqrt{3}$  structure on Au(111) then corresponds to 4.625 molecules  $\text{nm}^{-2}$ .

### 3. Irradiation induced beam damage of biomaterial surfaces

Beam damage of organic molecules is a major concern and was carefully investigated because self-assembled monolayers of organic molecules are susceptible to irradiation induced damage [18–21]. Irradiation generally results in loss of conformational order, appearance of dialkylsulfide species, partial dehydrogenation under formation of double bonds, and desorption of organic fragments [18, 22]. We characterized beam damage at both ambient pressure endstations of the advanced light source (ALS), Berkeley, USA. At beamline 11.0.2 (an undulator beamline), beam damage is rapid and in less than a minute the beam has induced the whole film to be damaged, as can be judged from the appearance of a new S 2p peak at 163.8 eV that is due to dialkylsulfide species (figure 3(a)) [23]. We followed the evolution of

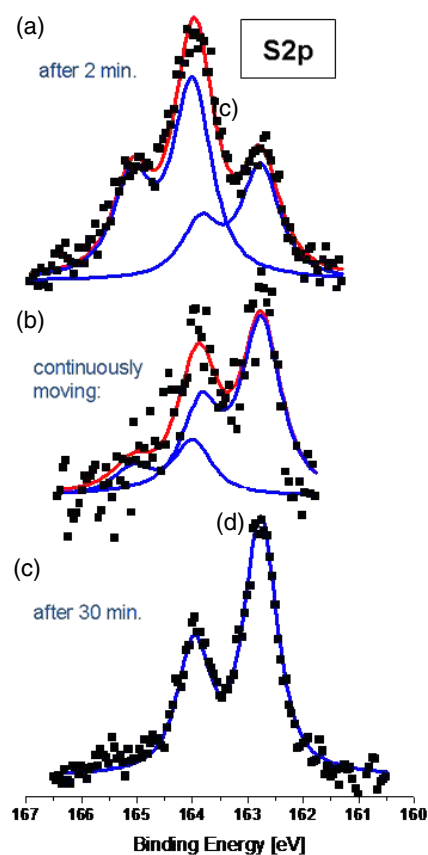


**Figure 3.** S 2p core level spectra of a self-assembled monolayer film (a) after 2 min irradiation at beamline 11.0.2 (accumulated exposure to  $4 \times 10^{14}$  photons  $\text{mm}^{-2}$ ), (b) during continuous movement with  $0.005 \text{ mm s}^{-1}$  at beamline 11.0.2 (accumulated exposure to  $2 \times 10^{14}$  photons  $\text{mm}^{-2}$ ), and (c) after 30 min irradiation at beamline 9.3.2 of the advanced light source, Berkeley (accumulated exposure to  $1.4 \times 10^{13}$  photons  $\text{mm}^{-2}$ ).

this new species over time by measuring the counts at fixed peak position of this peak (binding energy 163.8 eV). The plot in figure 4(a) shows the time evolution of the counts at 163.8 eV relative to the saturated value after long periods of exposure. Most of the film is destroyed in less than a minute exposure. Beam damage is a function of the incident photon flux (figure 4(b)). The spot size is on the order of 300  $\mu\text{m}$  diameter, and the flux during recording of the S 2p spectra was  $3.3 \times 10^{12}$  photons  $\text{s}^{-1} \text{ mm}^{-2}$ . However, even with the lowest flux settings, the film was destroyed completely within a few minutes.

Beam damage can also be observed in the C 1s region (figure 5). Upon exposure to synchrotron radiation, the COOH-group vanished within less than a minute as can be seen from the reduction of the high binding energy peak at 289.5 eV (from the carboxylate carbon atom) and the shoulder at 287 eV (from the carbon atom neighboring the carboxylate group). Upon extended exposure, the low binding energy C 1s core level at 285 eV became broader and showed a lower binding energy component, probably due to C=C double bonds [22].

In addition to reducing the incident photon flux, beam damage could be reduced by continuously moving the sample under the beam, thereby reducing the exposure time/ $\text{mm}^2$ .

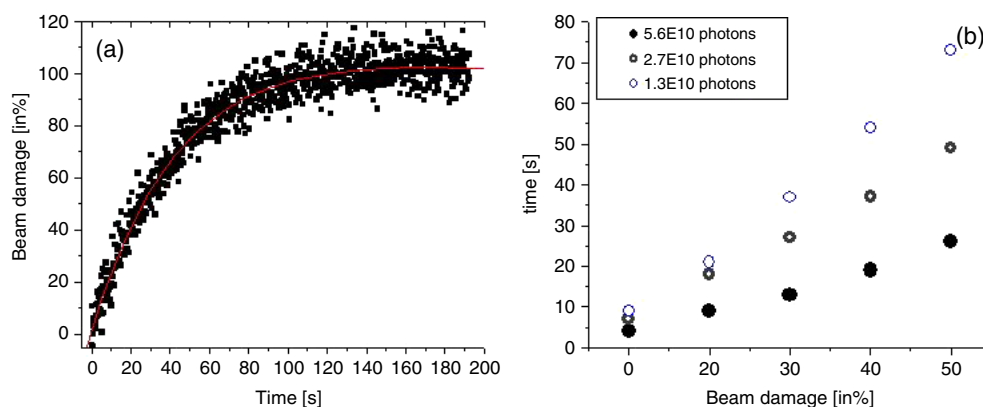


**Figure 4.** (a) S 2p core level spectrum of a COOH-terminated self-assembled monolayer on Au(111) under exposure. (b) Beam damage (in %) as a function of photon flux at the undulator beamline 11.0.2 of the ALS. The flux was decreased by closing the exit slit from 120  $\mu\text{m}$  to 60  $\mu\text{m}$  to 30  $\mu\text{m}$ .

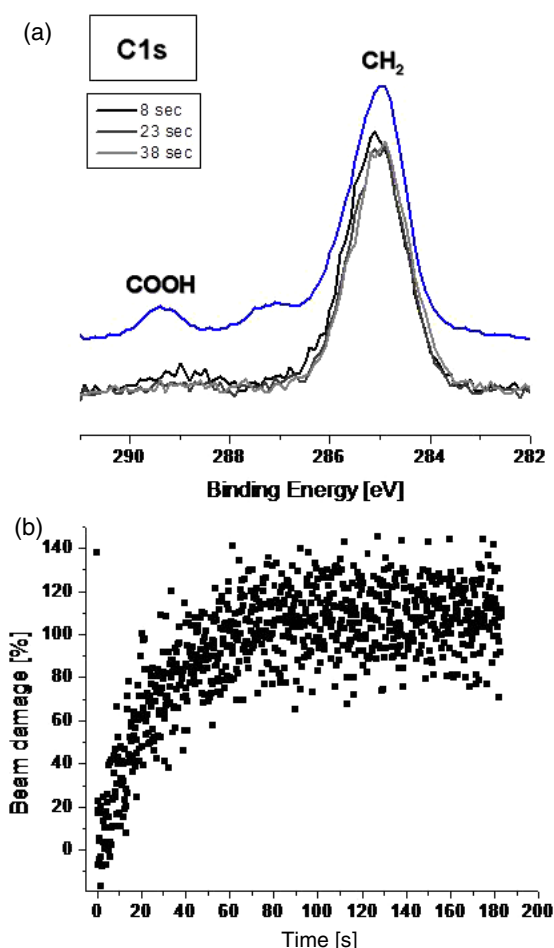


**Figure 5.** (a) C 1s core level spectrum of a COOH-terminated self-assembled monolayer on Au(111) under exposure of photons ( $1.7 \times 10^{14}$  photons  $\text{s}^{-1} \text{mm}^{-2}$ ) from beamline 11.0.2. (b) Plot of the intensity loss over time of the C 1s peak due to the COOH-functional group (a).

Figure 3(b) shows the S 2p region during continuous movement of the sample with  $0.005 \text{ mm s}^{-1}$  corresponding to an exposure of irradiated area for less than a minute. In this way, it is

possible to reduce the beam damage in the films to about 10% (figure 3(b)), at the expense of rapid consumption of unexposed surface area, long measurement times and worse signal-to-noise ratios.

Beam damage at the high flux undulator beamline 11.0.2 to the low flux bending magnet beamline 9.3.2 of the ALS is compared in figure 3(c). The flux of the bending magnet beamline 9.3.2 is two to three orders of magnitude lower than that of beamline 11.0.2 (about  $7.5 \times 10^9$  versus  $3.3 \times 10^{12}$  photons  $\text{s}^{-1} \text{mm}^{-2}$  for the S 2p core level). Even after 30 min exposure, there is only a single S 2p peak at the binding energy of intact thiols.

The beam damage at the ambient pressure beamlines of the ALS can be compared to irradiation induced damage at other third generation synchrotron facilities. At the undulator beamline I311 (Max II, Lund) with an estimated flux of  $4 \times 10^{13}$  photons  $\text{s}^{-1} \text{mm}^{-2}$  it has been found that only a few minutes destroy the film completely while beam damage at the bending magnet beamline D1011 with about 30 times less flux is much slower [23]. All water adsorption studies on SAMs were performed at beamline 9.3.2 with frequent moving to unexposed sample position (about every 20–30 min).

The POPC lipid films are affected in a similar way. We find a decrease of the C 1s intensity upon exposure, and an increase of the Si 2p substrate signal. However, the N 1s and P 2p core levels are much less affected than the C 1s core level, and in particular no change of the binding energy is observed. Thus, we assume that there is damage to the carbon chains and probably desorption of the lipid film.

## 4. Results

### 4.1. Water on functionalized self-assembled monolayers

The methyl-terminated SAM does not contain O atoms and thus shows no intensity under dry conditions. Up to 1 Torr water pressure (corresponding to a relative humidity of about 5%), no peak in the O 1s core level region could be discerned except for the gas phase water peak (figure 6). No change of the C 1s, S 2p, and Au 4f core level intensity and binding

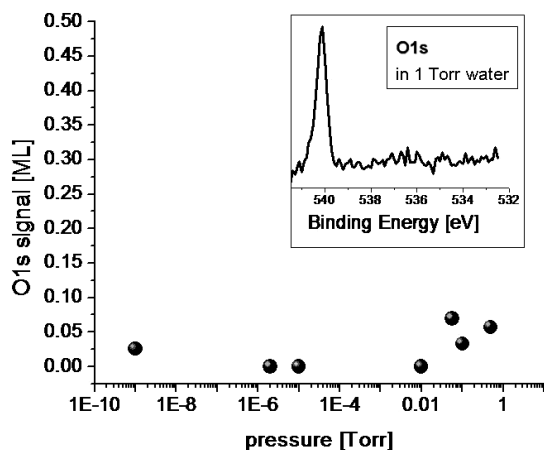


**Figure 6.** Normalized O 1s signal intensity of CH<sub>3</sub>-terminated SAM films as a function of water vapor pressure. The inset shows an O 1s core level spectrum in the presence of 1 Torr water (about 5% relative humidity). Except for the water gas phase peak at 540 eV, there is no O species present.

energy position is observed as a function of water pressure. As expected, this surface is hydrophobic and no water is adsorbed. We suppose that this is due to the absence of polar functional groups that can interact with the water molecule via, e.g., hydrogen bonding.

The O 1s core level of water is typically in the same energy range as O 1s core levels of the OH- and COOH-groups, which makes a direct quantitative analysis of the water coverage on functionalized thiol monolayers difficult. Figure 7 shows the procedure for extracting the O 1s intensity due to water adsorption on OH-terminated SAMs. We have used the C 1s and O 1s core levels (recorded with the same kinetic energy) of the dry SAM in ultrahigh vacuum as a reference to which spectra recorded in the presence of water can be normalized. When we normalize these two set of spectra to the same C 1s intensity (figure 7(a)), we can directly see the additional intensity that comes from water adsorption. No change of the C 1s core level is observed. The O 1s core level intensity has increased at the higher binding energy side of the O 1s peak. The binding energy for this species can be estimated to be between 533.0–534.0 eV. By subtracting the normalized O 1s spectra and normalizing the difference to the intensity of the dry spectrum (which corresponds to 1 ML of OH groups), we can estimate a water coverage of about 0.25 ML in the presence of 685 mTorr water.

In the presence of water vapor, the O 1s core level of the COOH-terminated film changes as can be seen in figure 8. In 100 mTorr water vapor, about 0.3 ML water are present on the surface as can be deduced from the total increase of the O 1s core level. The shape of the core level changes and there is a higher relative intensity of the higher binding energy core level, thus water adsorption contributes most strongly to the higher binding energy side of the spectrum. As both oxygen atoms in COOH are inequivalent on the timescale of the electron excitation, they produce two O 1s core levels at 532.3, and 533.7 eV. Both peaks are of similar intensity for fully protonated headgroups, for lower degrees of protonation,

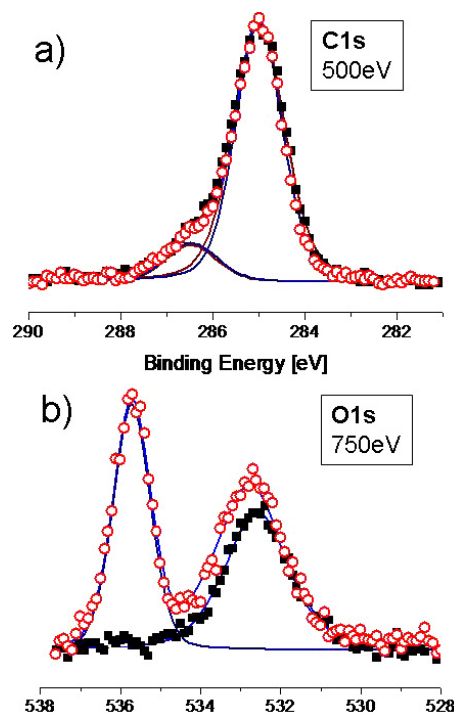


**Figure 7.** (a) C 1s and (b) O 1s core level in ultrahigh vacuum (filled squares) and in the presence of 685 mTorr water (open circles) at room temperature (about 3% relative humidity). The peak at 535.5 eV is due to gas phase water.

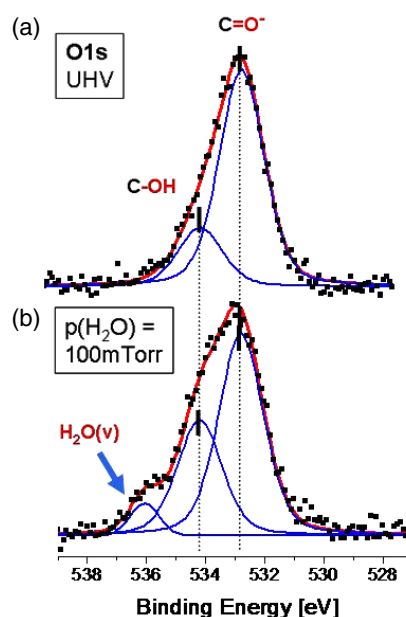


**Figure 8.** O 1s core level spectra of COOH-terminated SAMs in (a) ultrahigh vacuum, and (b) in the presence of 100 mTorr water vapor at room temperature (about 0.5% relative humidity), respectively (peak parameters were kept constant for the dry and wet film).

the O 1s spectrum appears asymmetric with a smaller high binding energy contribution. It is difficult to conclude whether the increase of the shoulder is solely due to water adsorption or whether it also is due to a higher degree of protonation.

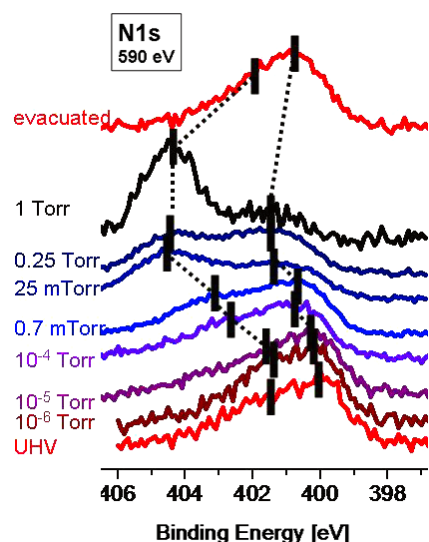


**Figure 9.** N 1s core level spectra (590 eV) as a function of increasing water vapor pressure, and after evacuation (from bottom to top). The shift of the peaks is shown by broken lines.

#### 4.2. Water interaction with phospholipid molecules

The POPC lipid molecule contains eight oxygen atoms in several different chemical states, and thus has a complex O 1s core level spectrum that is further complicated by the possible contribution of overlapping peaks from the silicon oxide substrate and water.

In order to study the interaction of water with the polar headgroup of the lipid molecules, we studied the much simpler N 1s and P 2p core levels instead. The N 1s core level is asymmetric with two maxima at binding energies of 400.1 and 401.7 eV under dry conditions (figure 9). These binding energies agree well with previously reported values for  $\text{NH}_3^+$  and  $\text{NH}_2$  in phospholipids, proteins and amino acids [16, 24], suggesting the presence of deprotonated and, to a lesser extent, protonated  $\text{NH}_2$ -groups in our experiment. With increasing water vapor pressure, the N 1s relative intensity of both peaks changed and the binding energy shifted to 401.4 and 404.3 eV, respectively. Binding energies up to 403.2 eV have been previously reported for phosphocholine lipids [25]. The unusually high binding energy shift observed in our experiments might be due to an additional contribution from H-bonded water.

Upon evacuation of the water, both N 1s core levels change back close to its original intensities and binding energies, showing that these changes are completely reversible.

The P 2p core level follows a similar trend (figure 10). Under dry conditions, there is one symmetric core level at 134.9 eV. This binding energy agrees well with previously reported P 2p core level from phosphocholine lipids [26] (values between 132.9 and 134.8 eV have been reported for different types of phospholipids) [24, 25, 27, 28]. This peak shifted by about 2 eV to higher binding energy in the presence of water vapor in the mTorr to Torr range. Upon evacuation, this peak shift was reversible close to the original spectral shape and position.

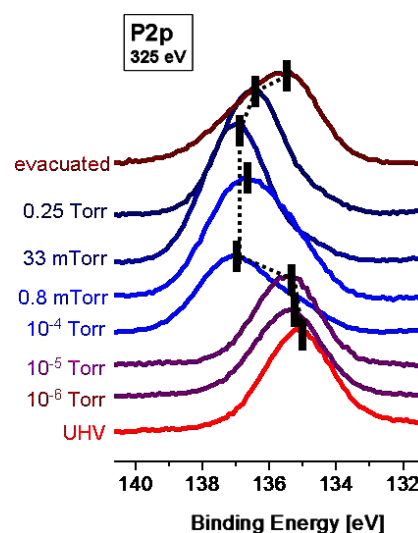


**Figure 10.** P 2p core level spectra (325 eV) as a function of increasing water vapor pressure, and after evacuation (from bottom to top). The shift of the peaks is shown by broken lines.

## 5. Discussion

The three different SAM films can be divided into hydrophobic ( $\text{CH}_3$ -terminated, no water adsorption), and hydrophilic ( $\text{OH}$ - and  $\text{COOH}$ -terminated) interactions with water. The hydrophilicity of organic molecules is clearly connected to the presence of polar headgroups. We were not able to adsorb water on the hydrophobic alkanethiol film. The  $\text{OH}$ -terminated films are hydrophilic and an equilibrium water layer with a coverage of 0.25 ML formed at room temperature in the presence of up to 1 Torr water. This corresponds to a relative humidity of about 5%.

Hydrophobic long chain alkanethiols on Au(111) have been depicted as suitable model compounds for the study of hydrophobic interactions with water based on their stability and cleanliness [29]. Polar headgroups are essential for H bonding and water adsorption. Monte Carlo simulations and sum frequency generation (SFG) experiments have shown hydrogen bonding to oxygen atoms of oligo(ethylene glycol)-terminated SAMs [30, 31]. Pyridine-terminated SAMs are strongly affected by water adsorption where H bonding and partial proton transfer was observed [32].

The presence of two distinct O peaks, at 532.8 and 534.2 eV binding energy in our case, in acid-terminated SAMs is expected from the different chemical state of the two O atoms in the  $\text{COOH}$ -groups. If the molecules were fully protonated the intensity of the two peaks should be equal. Clearly this is not the case and as can be seen in figure 8(b), the intensity of the peak from the protonated O atom is much smaller. This shows that our films exhibit a high degree of deprotonation. It has previously been observed that the degree of protonation changes when acetic acid was added to the ethanol solution from which the films were prepared [33]. A deprotonation of the carboxylic end group in the presence of a basic or ethanolic solution has been reported based on SFG measurements [34]. All these studies

have shown that H bonding and (de-)protonation reactions govern the interaction of water with organic functionalities. Our results therefore indicate that ambient pressure XPS is a well-suited technique to study these important phenomena, providing quantitative information of the degree of protonation and adsorption of water.

## 6. Conclusions

We have shown that the interaction of biomaterial surfaces with water is governed by polar functional groups that interact strongly with water molecules by hydrogen bonding. Provided that beam damage is carefully controlled, we demonstrate that *in situ* electron spectroscopy can give valuable information of the equilibrium amounts of adsorbed water layer, and on the bonding nature of the adsorbed water that are not accessible under ultrahigh vacuum conditions.

## Acknowledgments

This work was supported by the Director, Office of Energy Research, Office of Basic Energy Sciences, Chemical Sciences Division and Materials Sciences Division of the US Department of Energy, under contracts DE-AC03-76SF00098 and DE-AC02-05CH11231. Part of the work was performed at the Molecular Foundry. GK thanks the Max Planck Society for financial support.

## References

- [1] Israelichvili J and Wennerström H 1992 *Nature* **379** 219
- [2] Vogler E A 1998 *Adv. Colloid Interface Sci.* **74** 69
- [3] Love J C, Estroff L A, Kriebel J K, Nuzzo R G and Whitesides G M 2005 *Chem. Rev.* **105** 1103
- [4] Schreiber F 2000 *Prog. Surf. Sci.* **65** 151
- [5] Duwez A S 2004 *J. Electron Spectrosc. Relat. Phenom.* **97** 134
- [6] Ulman A 1996 *Chem. Rev.* **96** 1533
- [7] Nuzzo R G, Dubois L H and Allara D L 1990 *J. Am. Chem. Soc.* **112** 558
- [8] Bain C D and Whitesides G M 1989 *Angew. Chem. Int. Edn* **28** 506
- [9] Sackmann E 1996 *Science* **271** 43
- [10] Ottova-Leitmannova A and Tien H T 1992 *Prog. Surf. Sci.* **41** 337
- [11] Ogletree D F, Bluhm H, Lebedev G, Fadley C S, Hussain Z and Salmeron M 2002 *Rev. Sci. Instrum.* **73** 3872
- [12] Bluhm H *et al* 2006 *J. Electron Spectrosc. Relat. Phenom.* **150** 86
- [13] Yeh J J and Lindau I 1985 *At. Data Nucl. Data Tables* **32** 1
- [14] Heister K, Johansson L S O, Grunze M and Zharnikov M 2003 *Surf. Sci.* **529** 36
- [15] Pijpers A P and Meier R J 1999 *Chem. Soc. Rev.* **28** 233
- [16] Zubavichus Y, Fuchs O, Weinhardt L, Heske C, Umbach E, Denlinger J D and Grunze M 2004 *Radiat. Res.* **161** 346
- [17] Wen X, Linton R W, Formaggio F, Toniolo C and Samulski E T 2004 *J. Phys. Chem. A* **108** 9673
- [18] Zharnikov M and Grunze M 2002 *J. Vac. Sci. Technol. A* **20** 1793
- [19] Duwez A S 2004 *J. Electron Spectrosc. Relat. Phenom.* **97** 134
- [20] Graham R L, Bain C D, Biebuyck H A, Laibinis P E and Whitesides G M 1993 *J. Phys. Chem.* **97** 9456
- [21] Zerulla D and Chasse T 1999 *Langmuir* **15** 5285
- [22] Zharnikov M, Geyer W, Goelzhaeuser A, Frey S and Grunze M 1999 *Phys. Chem. Chem. Phys.* **1** 3163
- [23] Heister K, Zharnikov M, Grunze M, Johansson L S O and Ulman A 2001 *Langmuir* **17** 8
- [24] Lorusso G F, De Stasio G, Casalbore P, Mercanti D, Ciotti M T, Cricenti A, Generosi R, Perfetti P and Margaritondo G 1997 *J. Phys. D: Appl. Phys.* **30** 1794
- [25] Wang T, Wang Y Q, Su Y L and Jiang Z Y 2005 *Colloids Surf. B* **46** 233
- [26] Yang Z and Yu H 1999 *Langmuir* **15** 1731
- [27] Ye S H, Watanabe J, Iwasaki Y and Ishihara K 2005 *J. Membr. Sci.* **249** 133
- [28] He Q, Tian Y, Kuller A, Grunze M, Golzhauser A and Li J 2006 *J. Nanosci. Nanotechnol.* **6** 1838
- [29] Maccarini M, Himmelhaus M, Stoycheva S and Grunze M 2005 *Appl. Surf. Sci.* **252** 1941
- [30] Pertsin A J and Grunze M 2000 *Langmuir* **16** 8829
- [31] Wang R Y, Himmelhaus M, Fick J, Herrwerth S, Eck W and Grunze M 2005 *J. Chem. Phys.* **122** 164702
- [32] Zubavichus Y, Zharnikov M, Yang Y, Fuchs O, Umbach E, Heske C, Ulman A and Grunze M 2004 *Langmuir* **20** 11022
- [33] Willey T W, Vance A L, van Buuren T, Bostedt C, Nelson A J, Terminello L J and Fadley C S 2004 *Langmuir* **20** 2746
- [34] Methivier C, Beccard B and Pradier C M 2003 *Langmuir* **19** 8807